

PAPER • OPEN ACCESS

The impacts of fossil fuel emission uncertainties and accounting for 3-D chemical CO₂ production on inverse natural carbon flux estimates from satellite and *in situ* data

To cite this article: James S Wang *et al* 2020 *Environ. Res. Lett.* **15** 085002

View the [article online](#) for updates and enhancements.

Environmental Research Letters



PAPER

OPEN ACCESS

RECEIVED
17 February 2020

REVISED
8 May 2020

ACCEPTED FOR PUBLICATION
28 May 2020

PUBLISHED
21 July 2020

Original content from this work may be used under the terms of the [Creative Commons Attribution 4.0 licence](#). Any further distribution of this work must maintain attribution to the author(s) and the title of the work, journal citation and DOI.



The impacts of fossil fuel emission uncertainties and accounting for 3-D chemical CO₂ production on inverse natural carbon flux estimates from satellite and *in situ* data

James S Wang^{1,2,4} , Tomohiro Oda^{1,2} , S Randolph Kawa², Sarah A Strode^{1,2} , David F Baker³ , Lesley E Ott² and Steven Pawson² 

¹ Goddard Earth Science Technology and Research, Universities Space Research Association, Columbia, MD, United States of America

² NASA Goddard Space Flight Center, Greenbelt, MD, United States of America

³ Cooperative Institute for Research in the Atmosphere, Colorado State University, Fort Collins, CO, United States of America

⁴ Now at the Institute for Advanced Sustainability Studies, Potsdam, Germany

E-mail: james.s.wang@post.harvard.edu and toda@usra.edu

Keywords: carbon cycle, carbon dioxide, inverse modeling, fossil fuel emissions, atmospheric chemistry, remote sensing

Supplementary material for this article is available [online](#)

Abstract

Atmospheric carbon dioxide (CO₂) inversions for estimating natural carbon fluxes typically do not allow for adjustment of fossil fuel CO₂ emissions, despite significant uncertainties in emission inventories and inadequacies in the specification of international bunker emissions in inversions. Also, most inversions place CO₂ release from fossil fuel combustion and biospheric sources entirely at the surface. However, a non-negligible portion of the emissions actually occurs in the form of reduced carbon species, which are eventually oxidized to CO₂ downwind. Omission of this ‘chemical pump’ can result in a significant redistribution of the inferred total carbon fluxes among regions. We assess the impacts of different prescriptions of fossil fuel emissions and accounting for the chemical pump on flux estimation, with a novel aspect of conducting both satellite CO₂ observation-based and surface *in situ*-based inversions. We apply 3-D carbon monoxide (CO) loss rates archived from a state-of-the-art GEOS chemistry and climate model simulation in a forward transport model run to simulate the distribution of CO₂ originating from oxidation of carbon species. We also subtract amounts from the prior surface CO₂ fluxes that are actually emitted in the form of fossil and biospheric CO, methane, and non-methane volatile organic compounds (VOCs). We find that the posterior large-scale fluxes are generally insensitive to the finer-scale spatial differences between the ODIAC and CDIAC fossil fuel CO₂ gridded datasets and assumptions about international bunker emissions. However, accounting for 3-D chemical CO₂ production and the surface correction shifts the global carbon sink, e.g. from land to ocean and from the tropics to the north, with a magnitude and even direction that depend on assumptions about the surface correction. A GOSAT satellite-based inversion is more sensitive to the chemical pump than one using *in situ* observations, exhibiting substantial flux impacts of 0.28, 0.53, and -0.47 Pg C yr⁻¹ over tropical land, global land, and oceans, due to differences in the horizontal and vertical sampling of the two observation types. Overall, the biases from neglecting the chemical pump appear to be minor relative to the flux estimate uncertainties and the differences between the *in situ* and GOSAT inversions, but their relative importance will grow in the future as observational coverage further increases and satellite retrieval biases decrease.

1. Introduction

Top-down approaches for estimating greenhouse gas (GHG) fluxes, such as inverse modeling (Enting and

Mansbridge 1989), rely on atmospheric GHG measurements and information on atmospheric transport to quantify anthropogenic and/or natural sources and sinks at scales ranging from point sources and

cities (e.g. Lauvaux *et al* 2016, Nassar *et al* 2017, Gourdjji *et al* 2018) to sub-national and national entities (e.g. Manning *et al* 2011, Graven *et al* 2018, Liu *et al* 2018) to continents and the globe (e.g. Gurney *et al* 2002, Reuter *et al* 2014). There has been growing interest in employing flux inversions to support independent monitoring, reporting, and verification (MRV) of national and sub-national GHG emissions and sinks to complement the bottom-up inventories required under the UN Framework Convention on Climate Change (Leip *et al* 2018; <https://ig3is.wmo.int/en>, accessed 17 March 2019; IPCC 2019; <https://carbon.nasa.gov/>, accessed 17 March 2019). Inversions for estimating natural carbon fluxes help to provide insights into the capacity of the Earth system to remove anthropogenic additions of carbon to the atmosphere and its changes over time (Le Quéré *et al* 2015). Such analyses can also potentially be used to verify Agriculture, Forestry and Other Land Use (AFOLU) carbon dioxide (CO₂) emissions and sinks estimated through stock change approaches, though it could be challenging in many cases to separate the AFOLU contributions to inferred fluxes from those of unmanaged lands and fossil fuel combustion (IPCC 2019).

Given that we are in an era of increasingly abundant satellite GHG data and flux inversions using them, along with continuous evolution towards higher-resolution models (e.g. Houweling *et al* 2015, Crowell *et al* 2019), it is necessary to re-examine the impacts of various methodological assumptions for flux inversions, which historically had been conducted using relatively sparse networks of mostly surface-air observations. For example, inversions using CO₂ observations to estimate natural carbon fluxes typically do not allow for adjustment of fossil fuel CO₂ emissions (FFCO₂), simply prescribing them as if they are a known quantity based on the rationale that their uncertainties are smaller than those of natural fluxes at the coarse spatial scales of most global inversions (Gurney *et al* 2005, Peylin *et al* 2013). Given the significant spatial pattern differences among emission inventories (e.g. Oda *et al* 2018) and the often incorrect specification or even omission of international bunker fuel emissions (including shipping and aviation) in inversions (e.g. Peylin *et al* 2013), substantial errors could propagate to the inferred natural fluxes (Nassar *et al* 2010). But other than a study by Gurney *et al* (2005) that reported some sensitivity of inferred natural fluxes to the addition of seasonal and interannual variations to prescribed FFCO₂ emissions, there has been a lack of inversion analyses isolating the impacts of differences in emission inventories and assumptions about bunkers, especially in the context of satellite column measurements.

Also, most current inversions assume that CO₂ is released from fossil fuel combustion and biospheric sources entirely at the surface. In reality, ~ 1 Pg C yr⁻¹

of the emissions (cf a global net carbon flux, including fossil fuels, of ~ 5 Pg C yr⁻¹) occurs in the form of reduced carbon species, including carbon monoxide (CO) and volatile organic compounds (VOCs), which are eventually oxidized to CO₂ in the atmosphere downwind of the emissions. As noted by a number of previous studies (Enting and Mansbridge 1991, Enting *et al* 1995, Baker 2001, Folberth *et al* 2005, Suntharalingam *et al* 2005, Jacobson *et al* 2007, Nassar *et al* 2010, Chevallier *et al* 2017), omission of this ‘chemical pump’ (Suntharalingam *et al* 2005) can result in significant systematic errors in the model distribution of atmospheric CO₂. Furthermore, a subset of the studies (Enting and Mansbridge 1991, Enting *et al* 1995, Baker 2001, Suntharalingam *et al* 2005, Jacobson *et al* 2007, Chevallier *et al* 2017) found shifts in inferred total carbon fluxes among regions as a result, e.g. between the tropics and northern extratropics and between land and ocean. However, Suntharalingam *et al* (2005) noted that a dearth of surface measurement sites over tropical and Southern Hemisphere extratropical land areas may have limited the sensitivity of their inversion to the chemical pump in those regions. Chevallier *et al* (2017) explored the use of satellite column CO₂ observations instead of surface measurements in their analysis.

In this study, we assess the impacts of the aforementioned sources of error on posterior natural fluxes, with a novel aspect of conducting both satellite CO₂ observation-based and surface *in situ*-based inversions. We employ a relatively high-resolution, global, Bayesian synthesis inversion system, which has been previously applied to observations from the Greenhouse gases Observing SATellite (GOSAT) as well as *in situ* measurements to examine the different constraints on the spatial and interannual variability of fluxes provided by the two observation types (Wang *et al* 2018). Our hypothesis in the present study is that there would be regional differences in the effects of fossil fuel uncertainties and the chemical pump (consisting of 3-D chemical CO₂ production and a surface correction) on the GOSAT vs. *in situ* inversion due to differences in the horizontal and vertical sampling of the two observation types, with the satellite observations having greater sensitivity to processes occurring above the surface and greater overall sensitivity in the regions where they provide better coverage, such as tropical and southern land regions.

2. Methods

This study uses a number of modeling components and prior flux data sets developed at NASA Goddard Space Flight Center (GSFC) with support from the NASA Carbon Monitoring System (CMS) program, whose objective over the past decade has been to promote the development of frameworks for quantifying carbon stocks and fluxes built primarily upon NASA

observing systems and models that can potentially satisfy MRV requirements for policy and management purposes (<https://carbon.nasa.gov/>, accessed 17 March 2019). The CMS products used here include CASA-GFED terrestrial biospheric fluxes (described in section 2.1 of this paper), Open-source Data Inventory for Anthropogenic CO₂ (ODIAC) FFCO₂ emissions (section 2.2), a PCTM transport model-based, batch, Bayesian flux inversion system (section 2.1), and a new capability of including 3-D chemical CO₂ production and a surface correction in the inversion (section 2.3).

2.1. Flux inversion system

The inversion system used here has been described and evaluated in detail in the Wang *et al* (2018) paper. In brief, it involves a batch Bayesian synthesis inversion technique (which gives an exact solution to the flux optimization problem, subject to prior constraints) based on that used in the TransCom 3 (TC3) global CO₂ inversion intercomparisons (Gurney *et al* 2002, Baker *et al* 2006) and that of Butler *et al* (2010). Advances over the previous methods include higher spatial and temporal resolution for the flux optimization—108 land and ocean regions in total (figure S1a (available online at stacks.iop.org/ERL/15/085002/mmedia)) and 8-day intervals, and the use of individual flask-air observations and daily averages for continuous observations rather than monthly averages. The Parameterized Chemistry and Transport Model (PCTM) (Kawa *et al* 2004), with meteorology from the NASA Global Modeling and Assimilation Office (GMAO) MERRA reanalysis (Rienecker *et al* 2011), was run at a resolution of 2° latitude × 2.5° longitude and 56 levels up to 0.4 hPa, and hourly temporal resolution. Prior constraints include gridded, 3-hourly net ecosystem production (NEP) and fire carbon fluxes estimated by the Carnegie-Ames-Stanford-Approach (CASA) biogeochemical model coupled to version 3 of the Global Fire Emissions Database (GFED3) (Randerson *et al* 1996, van der Werf *et al* 2006, 2010; with updates described in Ott *et al* 2015), and gridded, monthly, climatological, measurement-based air-sea CO₂ fluxes from Takahashi *et al* (2009). The prescribed FFCO₂ emissions in the Wang *et al* (2018) study were from the 1° × 1°, monthly- and interannually-varying Carbon Dioxide Information Analysis Center (CDIAC) inventory (Andres *et al* 2012), but in the present study, we use emissions from ODIAC (described below in section 2.2) as the baseline and present results using CDIAC only in sensitivity analysis.

In both the previous and present study, we assimilated *in situ* atmospheric CO₂ observations from 87 flask and continuous measurement sites in the NOAA ESRL (Dlugokencky *et al* 2013, Andrews *et al* 2009) and Japan Meteorological Agency (JMA; Tsutsumi *et al* 2006) networks (figure S1a), and the

ACOS B3.4 filtered and bias-corrected retrieval of column-average CO₂ dry air mole fractions (XCO₂) from GOSAT-measured near infrared radiances (figure S1b; O'Dell *et al* 2012; Osterman *et al* 2013). And as in the previous study, our inversions span the period March 2009–September 2010 (with the focus starting from June 2009), which is sufficiently long for assessing the impacts of FFCO₂ uncertainties and the chemical pump on global inversions.

Inversion system components specific to the present study are described in the following subsections.

2.2. ODIAC fossil fuel emissions

ODIAC is a global, gridded FFCO₂ data product with 1 × 1 km, monthly resolution over land and 1° × 1°, annual resolution for international bunkers from year 2000 onward (Oda *et al* 2018); the data product is commonly used in flux inversions (e.g. Takagi *et al* 2011, Maksyutov *et al* 2013, Lauvaux *et al* 2016, Crowell *et al* 2019). It shares country-level estimates with CDIAC, another commonly used data set, but distributes emissions within countries differently and includes gridded international bunker emissions. Rather than distributing emissions based on population density as in CDIAC, ODIAC applies information such as power plant profiles (emissions intensity and geographical location) and satellite nighttime light observations to different fuel types. The resulting emission distribution is in better agreement with the US bottom-up inventory developed by Gurney *et al* (2009) than is CDIAC (Oda and Maksyutov 2011). Global total emissions in the ODIAC version used are 8.70 and 9.13 Pg C for 2009 and 2010.

Shipping and aviation total emissions are derived from CDIAC and distributed using ship and flight track data (Oda *et al* 2018). Global total emissions are 0.17 and 0.12 Pg C yr⁻¹ for shipping and aviation in 2009 and 0.18 and 0.13 Pg C yr⁻¹ in 2010. For the present study, a simple vertical distribution for the aviation emissions is implemented. The emissions are partitioned into three layers—surface–4 km (27%), 4–10 km (34%), and 10–13 km (39%)—based on the altitude distribution from the AERO2k 2002 aviation inventory (Eyers *et al* 2005).

In the present study, we use the 2017 version of ODIAC (ODIAC2017, 2000–2016, Oda and Maksyutov 2015), and degraded the resolution to 2° × 2.5° for use in our version of PCTM. Figure 1 shows maps comparing ODIAC and CDIAC emissions. Sizable differences due to the spatial modeling approaches can be seen in many areas of high emissions, such as the eastern U.S. and East Asia (figure 1(c)), although negative and positive differences tend to compensate each other within each of these regions, given the shared country-level data of ODIAC and CDIAC.

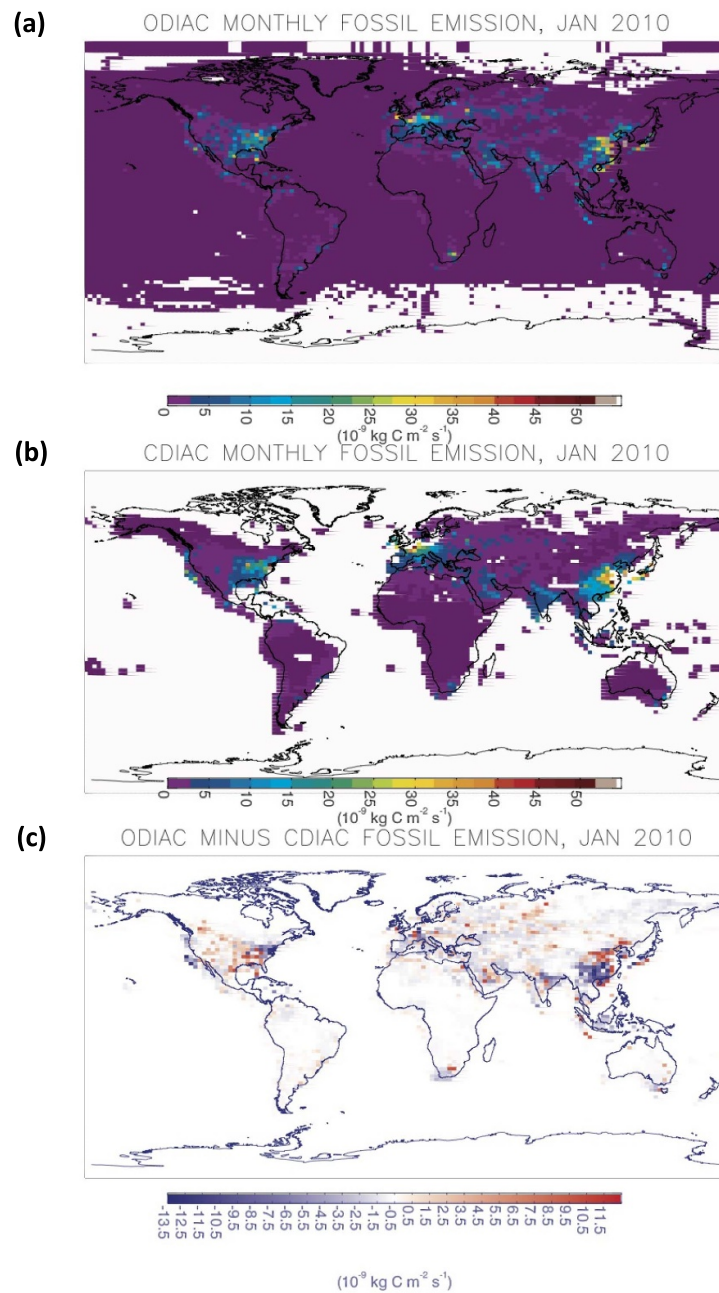


Figure 1. Fossil fuel CO_2 emissions on $2^\circ \times 2.5^\circ$ PCTM model grid for January 2010 from (a) ODIAC (including international shipping and aviation), (b) CDIAC, and (c) the difference between the data sets (ODIAC–CDIAC). (Land-based emissions inadvertently regridded into ocean grid cells have been redistributed to the nearest onshore grid cells as in the TC3 protocol (Gurney *et al* 2000).) Note that in (a), the more heavily traveled flight and ship tracks cannot be distinguished from the less traveled areas given the particular color scale, and in (c), the contributions of international shipping and aviation are not visible at all, since they fall within the white part of the color scale.

2.3. Atmospheric chemical CO_2 production and surface correction

We applied period-specific 3-D CO loss rates archived from a state-of-the-art NASA GEOS Chemistry and Climate Model (GEOSCCM; Oman *et al* 2013, Nielsen *et al* 2017) simulation in a forward PCTM

run to simulate the distribution of CO_2 originating from oxidation of reduced carbon compounds. Since CO is an intermediate product in most oxidation pathways for carbon compounds and the only significant product of its oxidation is CO_2 (Folberth *et al* 2005), its rate of loss through reaction with

Table 1. Chemical CO₂ production and surface correction budgets.

Component	Global, Annual Total (Pg C yr ⁻¹)		
	This work, 2009–2010 mean	Suntharalingam <i>et al</i> (2005), 1988–1997 mean	Nassar <i>et al</i> (2010), 2006
Total chemical production	1.15	1.10	1.05
Total surface correction	1.26 ^a	1.10	0.83
Fossil fuel combustion	0.28	0.30	0.38
Biomass and biofuel burning	0.23	0.34	0.00
Biospheric CH ₄	0.16	0.30	0.28
Biospheric NMVOCs	0.59	0.16	0.16

^aThis surface correction exceeds the chemical production because we apply, for simplicity, the entire amount of reduced carbon emissions rather than just the portion that is oxidized to CO. To compensate for the imbalance, we apply simple, small adjustments to the inversion flux results. See Supplementary Material for details.

hydroxyl (OH) radicals is approximately equal to the rate of production of CO₂. The GEOS simulation uses the comprehensive Global Modeling Initiative (GMI) stratospheric-tropospheric chemical mechanism, which includes O₃-NO_x-hydrocarbon interactions (Duncan *et al* 2007, Strahan *et al* 2007), and is nudged to meteorology from the latest reanalysis (MERRA-2; Gelaro *et al* 2017). From now on, we refer to the GEOS simulation as ‘MERRA2-GMI.’ Additional details on MERRA2-GMI are provided in the Supplementary Material. The MERRA2-GMI latitude-altitude distribution of CO loss rate (averaged over longitudes) for a selected month can be seen in figure 2(a), and a longitude-latitude cross-section at ~5 km altitude is shown in figure 2(b). CO oxidation (and thus CO₂ production) is greatest where OH oxidant is most abundant, i.e. in the tropics, and where CO concentrations are highest, e.g. downwind of biomass burning regions. The global total chemical CO₂ production is 1.15 Pg C yr⁻¹, similar to that of previous studies (table 1).

To accurately simulate the impact of the chemical pump, it is necessary to also subtract amounts of CO₂ at the surface actually emitted in the form of fossil and biospheric CO, CH₄, and non-methane VOCs (NMVOCs). Suntharalingam *et al* (2005) provide a thorough explanation of the purpose of the surface correction. Although errors in surface CO₂ fluxes can be corrected to a certain extent by the inversion, applying the chemical pump surface correction helps to minimize bias in the prior estimate, and thus strengthen the validity of a fundamental assumption

of Bayesian inversion (i.e. unbiased, Gaussian errors). Some other inversion analyses have neglected this prior correction while accounting for 3-D CO₂ production (Baker 2001, Chevallier *et al* 2017), relying on the inversion to make the necessary adjustments in surface fluxes; Baker (2001) then adds non-CO₂ emissions on to regional carbon budgets *a posteriori*. For the fossil fuel CO and NMVOC and biospheric NMVOC sources, we adopt the emissions fields from MERRA2-GMI, which promotes consistency between the surface correction and the chemical CO₂ production. Details on these and the other components of the surface correction are provided in the Supplementary Material. Global, annual totals are shown in table 1.

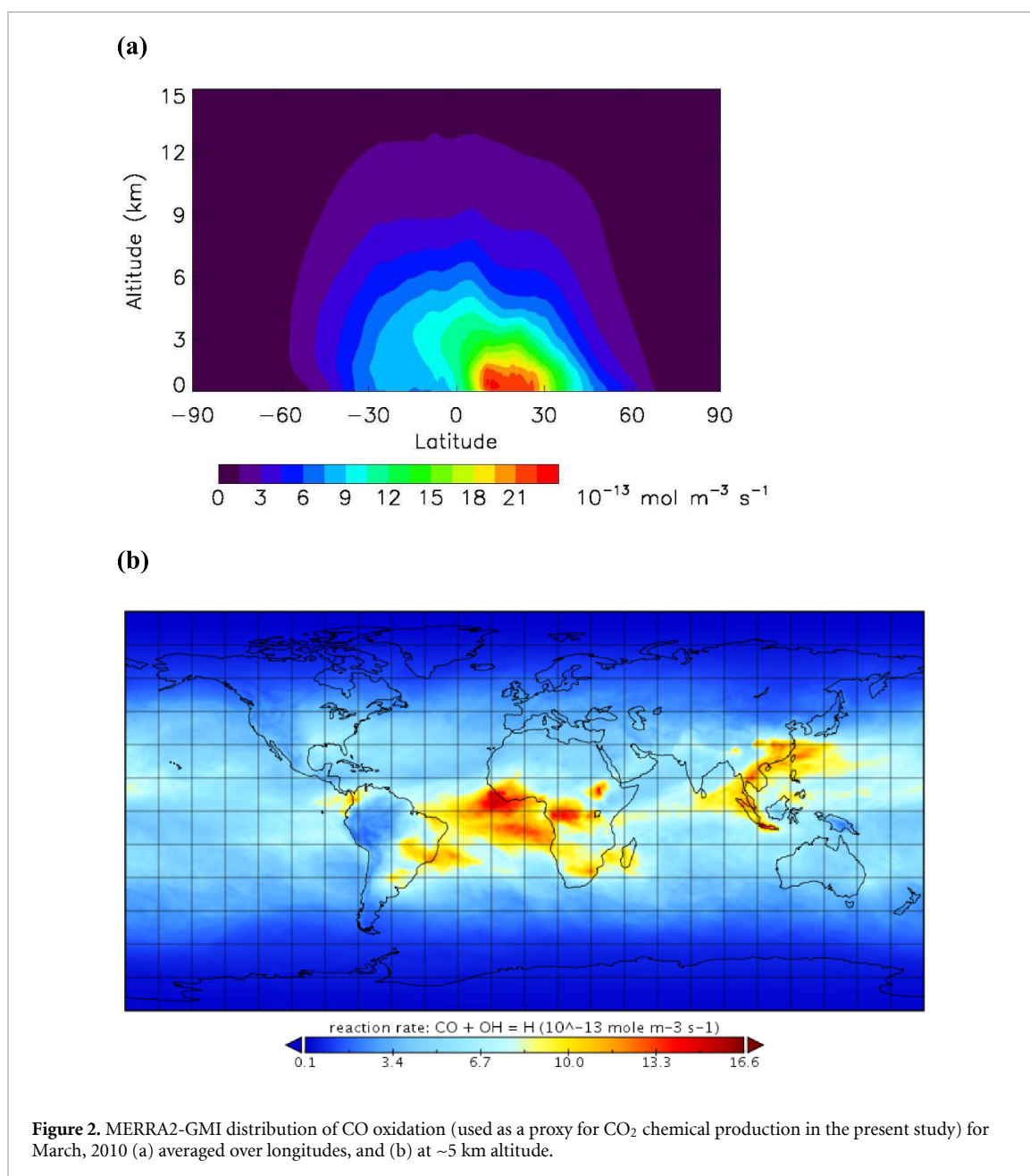
One important difference in this surface correction compared to those of previous studies is a much larger relative contribution from biospheric NMVOCs, i.e. 47% of the total vs. 15% and 19% (table 1), which places more of the surface correction at lower latitudes. A possible reason for the difference is that isoprene emissions are likely overestimated in GMI compared to that of, e.g. Guenther *et al* (1999, 2000). Another difference is the smaller contribution from CH₄ due to our exclusion of ruminants and landfills, which also de-weights higher latitudes. Yet another difference is that our fossil fuel correction is smaller overall and weighted more towards developing countries than that of Nassar *et al* (2010), which was a globally uniform percentage of FFCO₂ emissions.

The atmospheric concentrations of CO₂ attributable to CO₂ chemical production and to the surface correction simulated by PCTM after a year of production/subtraction and transport are shown in figure 3 for illustrative purposes (similar to figures 3 and 4 of Suntharalingam *et al* 2005). Figures 3(a) and (b) show the impact for the model surface layer, and figures 3(d) and (e) are for the atmospheric column average. Figure 3(c)/(f) show the net effect of chemical production and surface correction in the surface layer/column. As expected, the surface correction has a stronger effect on surface concentrations than on the column average, and is less dominant over chemical production in the column average as compared to the surface concentrations.

3. Results

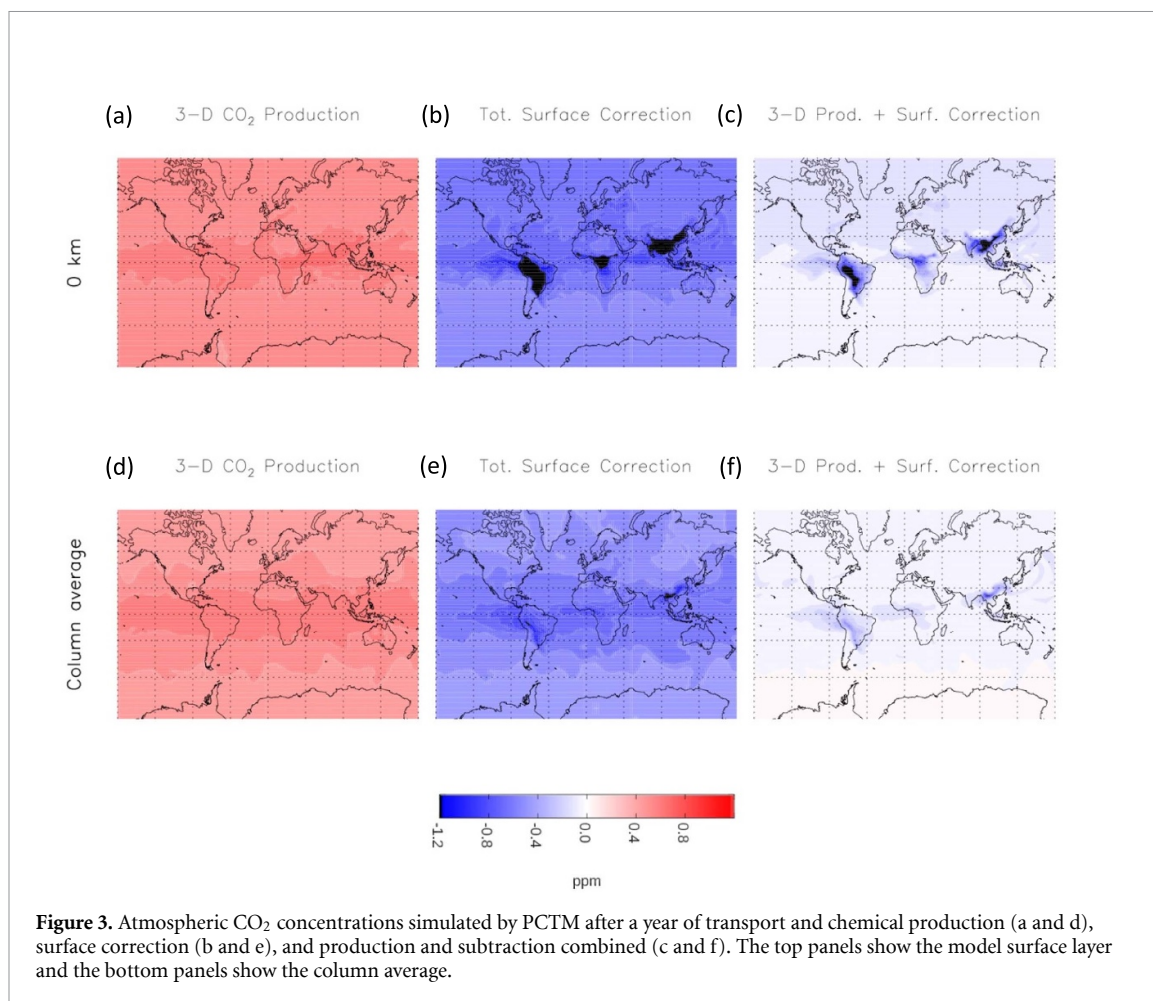
3.1. Impact of FFCO₂ spatial disaggregation differences on inversions

Inversions using either ODIAC FFCO₂ emissions, excluding the international bunkers, or CDIAC FFCO₂ emissions produce similar natural flux estimates in general, at least at the large spatial and temporal scales (e.g. sub-continental and seasonal) that are most relevant for the global carbon budget. Differences in estimated fluxes when GOSAT data are used in the inversions are within 0.25 Pg C yr⁻¹ (in absolute value) at the scale of large, aggregated



regions (e.g. northern land, tropical oceans) and seasons; twelve-month means are shown in figure 4. Inversions using *in situ* data exhibit some noticeably larger differences, even at the scale of these large-aggregate regions and twelve-month means; for example, ODIAC results in a $0.30 \text{ Pg C yr}^{-1}$ larger inferred source for southern land than does CDIAC, and a $0.28 \text{ Pg C yr}^{-1}$ weaker sink for northern oceans (figure 4). For individual seasons, differences for the *in situ* inversions are as large as 1 Pg C yr^{-1} (not shown). However, the differences are probably mostly noise rather than real differences in inferred natural fluxes at these large scales; Wang *et al* (2018) found the *in situ* inversion to be much noisier than the GOSAT inversion, with large temporal fluctuations, fewer degrees of freedom for signal, and more extensive flux error correlations,

reflecting insufficient constraints on the flux estimation provided by the relatively sparse *in situ* observations. In the FFCO₂ sensitivity results here, fluctuations in the differences between ODIAC- and CDIAC-based *in situ* inversions can be seen from season to season, as well as compensation between neighboring TC3 regions, e.g. ODIAC-CDIAC values of 0.52 and $-0.33 \text{ Pg C yr}^{-1}$ for Temperate Asia and Tropical Asia in DJF 2009–2010 and -2.37 and $1.47 \text{ Pg C yr}^{-1}$ for Temperate Asia and Boreal Asia in JJA 2010, likely reflecting negative error correlations. The GOSAT inversions do not exhibit similar fluctuations and compensation. An explanation for the noisy impact of FFCO₂ in particular is that the ODIAC and CDIAC emissions are distributed differently relative to the surface observation sites, some of which are located close to areas of high FFCO₂



emissions. Given that the sensitivity to surface fluxes, or ‘footprint,’ of surface observations can be rather localized and can vary greatly with meteorological conditions, a shift in prescribed FFCO₂ emissions could strongly and variably affect the fluxes inferred by certain sites, and for a sparse observation network, the impact could be substantial even when aggregated to large spatial scales. The GOSAT column observations, in contrast, are influenced by broader areas of surface fluxes, and the GOSAT data set provides better coverage than the *in situ* data set over many regions. Thus, the GOSAT inversion is not as sensitive to detailed spatial patterns of FFCO₂ emissions.

3.2. Impact of international bunker emissions

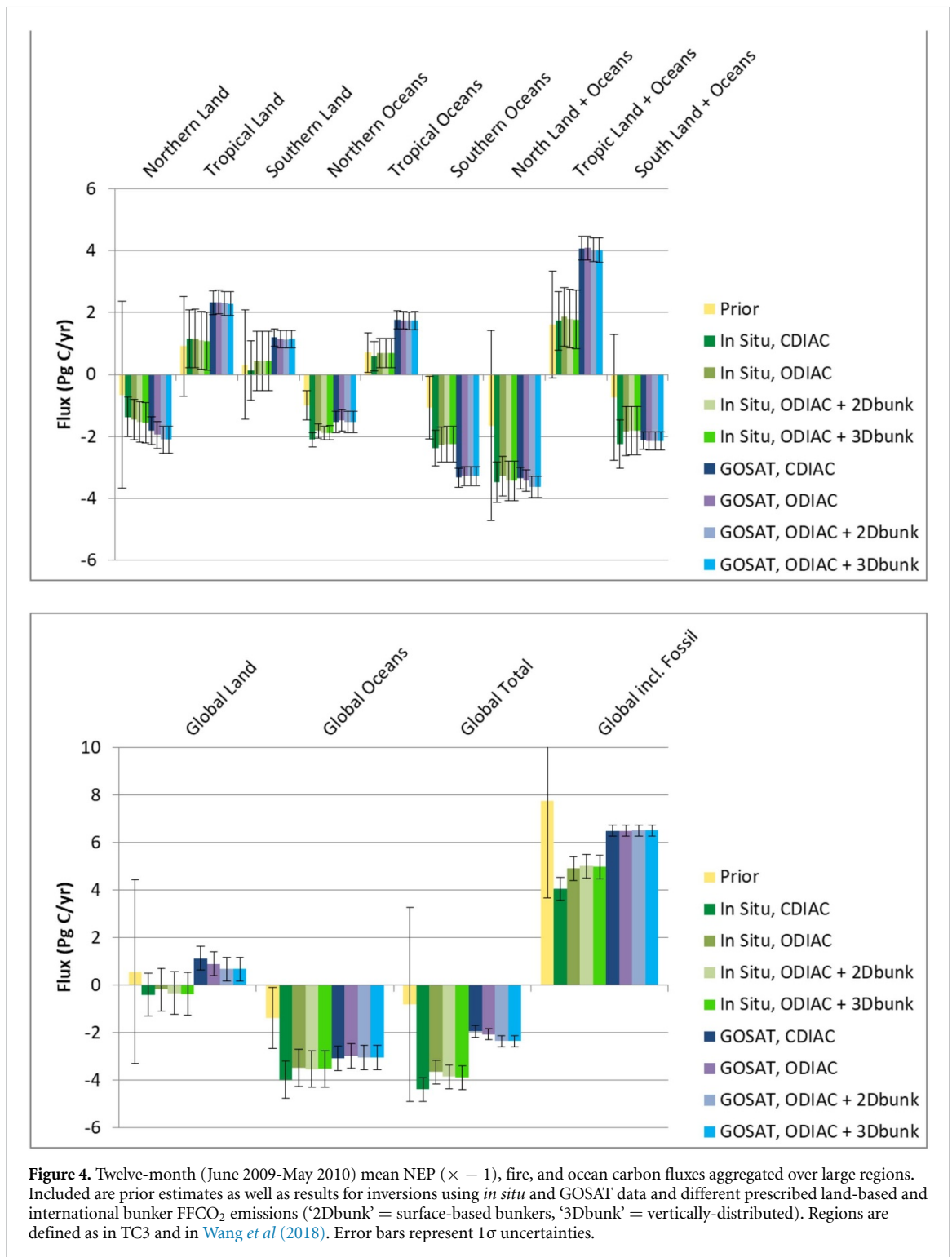
We also examined the impacts on inversions of accounting for international bunker FFCO₂ emissions and vertically distributing international aviation emissions. Figure 4 shows *in situ* and GOSAT aggregated posterior fluxes when international bunkers are included, either placed entirely at the surface or distributed over flight altitudes, next to results based on only land-based ODIAC FFCO₂. The differences are small, especially between the inversions with 2-D vs. 3-D bunkers. The impact of bunkers is most noticeable in the north (as that is where there is the most maritime and air traffic), where inclusion of

bunkers results in inferred fluxes that are more negative by up to 0.16 Pg C yr⁻¹ over land and 0.07 Pg C yr⁻¹ over ocean regions. (Global mass balance requires that larger FFCO₂ emissions be balanced by larger natural sinks.) The impact of vertically distributing aviation emissions is nearly imperceptible, with the largest impact being a decrease in the net source of 0.03 Pg C yr⁻¹ over tropical land in the *in situ* inversion.

We examine the posterior fit of the inversions to observations to assess whether that could provide an objective rationale for accounting for bunker emissions in CO₂ inversions. Results are presented and discussed in detail in the supplementary material. We find that the posterior fit differs little between the cases with and without bunkers for either the *in situ* or GOSAT inversions.

3.3. Impact of chemical pump

Results for inversions accounting for atmospheric chemical CO₂ production and the surface correction are shown alongside those for inversions without the chemical pump in figure 5. (All of the inversions are based on ODIAC land-based and vertically-distributed bunker emissions.) Notable features include larger net carbon sources over



tropical land and southern land when the chemical pump is included, larger net sinks or smaller net sources over ocean regions, and overall shifts in the global sink from the tropics to the north and, for the GOSAT inversions, from land to ocean. The effects can generally be explained by mass balance considerations—e.g. CO₂ production downwind of continental reduced carbon emissions necessitates more CO₂ uptake over ocean regions to fit observations, and surface corrections that are especially

large over tropical and southern land necessitate more CO₂ emissions over those regions. The more negative oceanic flux is consistent with what was found in the previous inversion study by Suntharalingam *et al* (2005). However, the increased source over tropical land (and lack of flux adjustment over northern land) is different from the decreased tropical land source and decreased northern land sink of Suntharalingam *et al* (2005) and Jacobson *et al* (2007). Our analysis suggests this is due to differences in our

surface corrections, as discussed in detail later in this section.

The GOSAT inversion is more sensitive to the chemical pump than the *in situ* inversion in general, exhibiting relatively large twelve-month mean impacts of 0.28, 0.53, and -0.47 Pg C yr⁻¹ over tropical land, global land, and global oceans; these are changes of 12%, 78%, and 15% relative to the posterior net sources/sinks. Note, however, that the impacts all lie within or close to the 1σ uncertainty ranges of the flux estimates. For comparison, the inversions of Suntharalingam *et al* (2005) (based on *in situ* observations) exhibited impacts of 0.10 and -0.09 Pg C yr⁻¹ over global land and global oceans (averaged over multiple models). The differences between the *in situ* and GOSAT inversions are consistent with differences between the data sets in horizontal and vertical sampling. Some insight can be gained by examining the impact of the chemical pump on atmospheric CO₂ concentrations averaged over the locations and times of the *in situ* and GOSAT observations (table 2). The numbers, though of small magnitude, exhibit particular patterns. For example, the GOSAT sampling exhibits values that are more positive (or less negative) for ocean overall and in some of the zones, i.e. 0°–30°N and 30°–60°N, than the *in situ* sampling does. This reflects the greater sensitivity of the column observations to chemical CO₂ production, which occurs over a range of altitudes above the surface downwind of continents (figures 2(a) and (b)), and can explain the larger negative flux adjustments over oceans in the GOSAT inversion in response to the chemical pump. Also, the GOSAT combined land-ocean impacts are weighted towards the land values in all zones except for 60°–30°S, reflecting a much larger number of land nadir than ocean glint observations (figure S1b), whereas the *in situ* combined impacts are weighted towards land only outside of the tropics, reflecting the dearth of land sites in the tropics (figure S1a). This could explain the lack of flux adjustments over tropical and southern land in the *in situ* inversions in response to the land-based surface correction.

We examine the posterior fit of the inversions to observations for the cases with and without the chemical pump also. (See the Supplementary Material for details.) We find that the posterior fit generally differs little between the cases.

Since our surface corrections differ in important ways from those assumed in previous studies, we also examine results of an alternative set of inversions using surface corrections that are more similar to those of previous studies. Specifically, the global, annual magnitude of the correction for biospheric NMVOCs is the same as that of Suntharalingam *et al* (2005) and Nassar *et al* (2010), rather than much larger as with our baseline correction (table 1). In addition, the fossil fuel correction is based on the uniform 4.89% scaling of Nassar *et al* (2010), which makes it

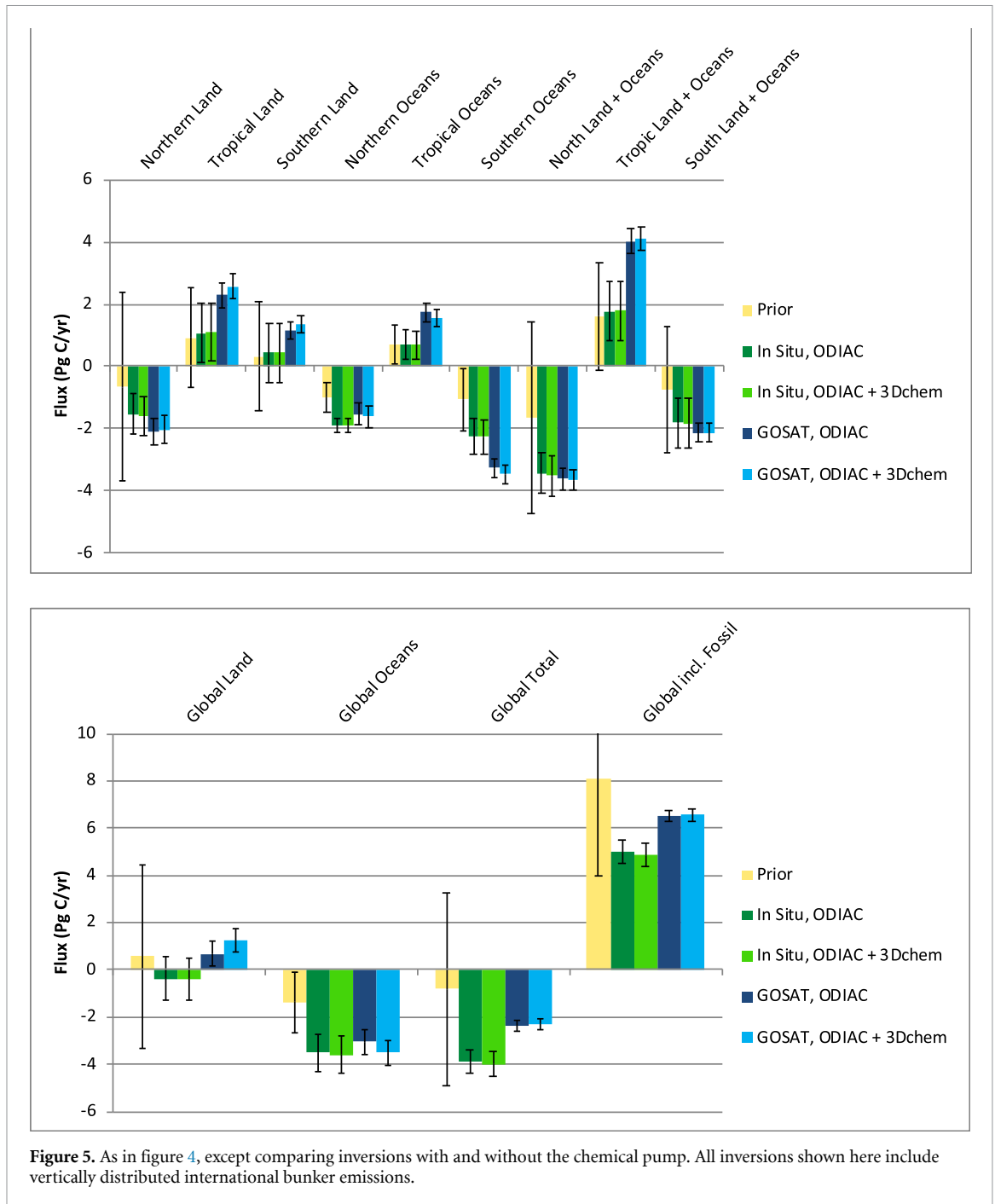
much larger over developed countries (located mostly in the north) and smaller over developing countries and possibly more similar to that of Suntharalingam *et al* (2005), whose earlier study period may have occurred before emissions controls greatly reduced the proportion of incomplete combustion products in developed countries. These alternative surface corrections result in a chemical pump impact on atmospheric CO₂ with a north-south interhemispheric difference of -0.23 ppm sampled at *in situ* sites, which is quite different from the -0.07 ppm of our baseline experiment and more similar to the -0.20 ppm of Suntharalingam *et al* (2005) (though the networks of *in situ* sites are not exactly the same). Accounting for this version of the chemical pump shifts a portion of the global CO₂ sink from the north to the tropics and south, as in previous studies (figure S3). Unchanged from our baseline inversions is the overall shift in the sink from land to oceans in the GOSAT inversion. Thus, regional flux shifts are sensitive to the surface correction, and differences in the correction appear to explain the contrasting latitudinal shifts in our analysis and previous studies.

4. Discussion and conclusions

Here, we present an assessment of the impact of several types of prior emissions errors on land and ocean carbon fluxes estimated through atmospheric inversions. Unlike previous studies, we consider both surface and satellite data inversions. As the international community seeks to use inverse methods and an international constellation of carbon observing satellites in support of emissions MRV, evaluating the potential of such uncertainties to influence inferred fluxes is critically important.

Our results show that large-scale natural fluxes in a global inversion are not substantially affected by differences between two commonly used sets of prescribed FFCO₂ emissions, ODIAC and CDIAC, though we do see noise in the *in situ* inversion results that is probably an artifact of the sparseness of the observation network combined with the location of some of the sites close to large FFCO₂ emissions. Inferred fluxes can exhibit larger impacts in relative terms at smaller spatiotemporal scales, this being especially relevant for higher-resolution regional-scale inversions. We should also point out that the differences between ODIAC and CDIAC may not be as large as those between other data sets, such as EDGAR vs. CDIAC (Oda *et al* 2018), given that the two share country-level estimates. Note that evaluating whether one of the FFCO₂ data sets is more accurate than the other was not one of the objectives of this study.

The small impacts on inversions of including international bunker emissions and vertically distributing the aviation portion are not all that surprising, given the relatively small amounts of the



emissions, making up around 3% of global FFCO₂. This finding should provide reassurance that imprecise treatment of bunker emissions by past and ongoing inversion studies has not been significantly biasing results.

Accounting for 3-D chemical CO₂ production and surface corrections results in sizable shifts in sources and sinks between some regions, especially in the inversions using GOSAT column-average data, with, most notably, increased sources of 0.28 and 0.53 Pg C yr⁻¹ over tropical and global land and an increased ocean sink of 0.47 Pg C yr⁻¹. An important difference between our results and those of the most similar, previous inversion studies is the

direction of the latitudinal shift in global sink, with our baseline analysis indicating a shift from the tropics to the north. Our investigation suggests that the difference can be attributed to differences in the surface correction we apply, which in turn suggests a need to better constrain the distribution of non-CO₂ carbon emissions from fossil fuel and biospheric sources. Even with the qualitatively different and relatively large flux shifts in our study, the chemical pump effects lie mostly within the 1 σ uncertainty ranges of the flux estimates though, and are generally much smaller than the differences between the *in situ* and GOSAT inversions (figure 5). But it is worth keeping in mind that common assumptions in

Table 2. Impact of chemical pump (chemical production–surface correction) on atmospheric CO₂ averaged over different domains as sampled by surface and satellite observations (June 2009–May 2010 mean).

Domain		<i>In situ</i> obs (ppm)	GOSAT obs (ppm) ^a
90°–60°S	land	0.004	—
	Ocean	—	—
	Combined	0.004	—
60°–30°S	land	–0.004	–0.020
	Ocean	0.001	–0.018
	Combined	–0.002	–0.019
30°–0°S	land	–0.108	–0.033
	Ocean	–0.022	–0.030
	Combined	–0.052	–0.032
0°–30°N	land	–0.091	–0.050
	Ocean	–0.075	–0.032
	Combined	–0.077	–0.045
30°–60°N	land	–0.124	–0.022
	Ocean	–0.075	0.006
	Combined	–0.120	–0.021
60°–90°N	land	–0.061	0.004
	Ocean	–0.047	—
	Combined	–0.057	0.004
Global	land	–0.111	–0.031
	Ocean	–0.064	–0.028
	Combined	–0.097	–0.030

^aModel profiles are weighted using ACOS column averaging kernels.

flux inversions that are known to be incorrect, such as emitting reduced carbon as CO₂ at the surface, can cause definite biases in inferred natural fluxes with regional patterns. As posterior flux uncertainties decrease with greater coverage by *in situ* and satellite observations (from geostationary Nivitanont *et al* 2019 as well as low-Earth orbit platforms; Eldering *et al* 2017) and satellite retrieval biases continue to decrease in the future (with potentially active as well as passive measurement techniques; ASCENDS Ad Hoc Science Definition Team 2015), biases due to neglecting the chemical pump will increase in relative importance.

The above considerations provide another rationale for synergistic use of multiple species for carbon budget analysis (Palmer *et al* 2006). Specifically, current and future satellite (e.g. GOSAT-2; Imasu 2019) and surface observations of species such as CO, CH₄, and NMVOCs in addition to CO₂ could be used in joint inversions to simultaneously optimize surface fluxes of the different species and 3-D chemical CO₂ production, extending the CO data assimilation work of Nassar *et al* (2010). This could provide better constraints on the global carbon cycle than can be achieved with CO₂ observations alone. Once fundamental issues in inversions such as observation biases and coverage gaps have been better addressed, joint inversions do offer the promise of reducing uncertainties even in OH distributions, given that tracer observations can be used to constrain sinks as well as sources (as in the CH₄ inversions of Wang *et al* 2004) and that the CO sink due to OH is essentially perfectly correlated with the chemical production source of CO₂.

Acknowledgments

This work has been supported by the NASA Atmospheric CO₂ Observations from Space program element, the NASA Carbon Monitoring System Program, and the NASA Carbon Cycle Science program (Grant No. NNX14AM76G, PI: T. Oda). The NASA Goddard High-End Computing Program and the Atmospheric Chemistry and Dynamics Laboratory provided access to supercomputing resources at the NASA Center for Climate Simulation and the GSFC Code 614 cluster, respectively. We are grateful to Ilan Chabay, Mark Lawrence, and Ortwin Renn at the IASS and Achim Maas and Judith von Pöggel in the IASS Fellowship program for travel funding to present the work at the 2019 EGU conference and for the time and space to finish work on the manuscript. Thanks go to Luke Oman for leading the production of the MERRA2-GMI simulation and making the results available. The ACOS GOSAT data were produced by the ACOS/OCO-2 project at the Jet Propulsion Laboratory, California Institute of Technology using spectra acquired by the GOSAT Project. We thank Chris O'Dell for providing the ACOS data to us, Luciana Gatti, John Miller, and Manuel Gloor for providing the Amazonica data, NOAA ESRL GMD CCGG for making their flask and continuous tower data publicly available, and JMA (including Yukio Fukuyama and Atsushi Takizawa) for making their *in situ* data publicly available on the WDCGG website. And many thanks go to G. James Collatz for providing CASA-GFED fluxes, Prabir Patra for CH₄ emissions, Michael Manyin for modeling help, Martha Butler for inversion code and

documentation, and Stephen Steenrod for computing help.

Data availability

The MERRA2-GMI simulation output that supports the findings of this study is openly available at https://opendap.nccs.nasa.gov/dods/merra2_gmi/ and also at https://portal.nccs.nasa.gov/datashare/merra2_gmi/.

The ODIAC2017 data product that supports the findings of this study is openly available from the data server hosted by the National Institute for Environmental Studies, <http://db.cger.nies.go.jp/dataset/ODIAC/>, 10.17595/20170411.001.

The 3-D chemical CO₂ production and surface correction data that support the findings of this study are available from the corresponding authors upon reasonable request.

ORCID iDs

James S Wang  <https://orcid.org/0000-0003-1713-8420>

Tomohiro Oda  <https://orcid.org/0000-0002-8328-3020>

Sarah A Strode  <https://orcid.org/0000-0002-8103-1663>

David F Baker  <https://orcid.org/0000-0003-4144-4946>

Steven Pawson  <https://orcid.org/0000-0003-0200-717X>

References

- Andres R J, Boden T A and Marland G 2012 *Monthly Fossil-Fuel CO₂ Emissions: Mass of Emissions Gridded by One Degree Latitude by One Degree Longitude*, Carbon Dioxide Information Analysis Center, Oak Ridge National Laboratory (Oak Ridge, TN: U.S. Department of Energy); see also (<https://data.ess-dive.lbl.gov/view/doi:10.3334/CDIAC/FE.MONTHLYMASS.2016>)
- Andrews A E, Kofler J, Bakwin P S, Zhao C and Tans P 2009 Carbon Dioxide and Carbon Monoxide Dry Air Mole Fractions from the NOAA ESRL Tall Tower Network, 1992–2009, version: 2011-08-31, Path: (ftp://aftp.cmdl.noaa.gov/data/trace_gases/co2/in-situ/tower/)
- ASCENDS Ad Hoc Science Definition Team 2015 Active Sensing of CO₂ Emissions over Nights, Days, and Seasons (ASCENDS) Mission Science Mission Definition Study (draft) available at: https://cce.nasa.gov/ascends_2015/ASCENDS_FinalDraft_4_27_15.pdf (accessed 11 August 2017)
- Baker D F 2001 Sources and Sinks of Atmospheric CO₂ Estimated from Batch Least-Squares Inversions of CO₂ Concentration Measurements, *Ph.D. dissertation*, Princeton University, January 2001
- Baker D F, Law R M, Gurney K R, Rayner P and Peylin P and co-authors 2006 TransCom 3 inversion intercomparison: Impact of transport model errors on the interannual variability of regional CO₂ fluxes, 1988–2003 *Glob. Biogeochem. Cycles* **20** GB1002
- Butler M P, Davis K J, Denning A S and Kawa S R 2010 Using continental observations in global atmospheric inversions of CO₂: North American carbon sources and sinks *Tellus* **62B** 550–72
- Chevallier F, Zheng B and Ciais P 2017 Assessment on the possibility to account for the 3D production of CO₂, ECMWF Copernicus Report No. D73.4.5.2-2017, CAMS73_2015SC2_D73.4.5.2-2017_201704_3D production CO₂_v1
- Crowell S et al 2019 The 2015–2016 carbon cycle as seen from OCO-2 and the global in situ network *Atmos. Chem. Phys.* **19** 9797–831
- Dlugokencky E J, Lang P M, Masarie K A, Crotwell A M and Crotwell M J 2013 Atmospheric Carbon Dioxide Dry Air Mole Fractions from the NOAA ESRL Carbon Cycle Cooperative Global Air Sampling Network, 1968–2012, version: 2013-08-28, available at: ftp://aftp.cmdl.noaa.gov/data/trace_gases/co2/flask/surface/ (accessed 18 February 2014)
- Duncan B N, Strahan S E, Yoshida Y, Steenrod S D and Livesey N 2007 Model study of the cross-tropopause transport of biomass burning pollution *Atmos. Chem. Phys.* **7** 3713–36
- Eldering A et al 2017 The Orbiting Carbon Observatory-2 early science investigations of regional carbon dioxide fluxes *Science* **358** eaam5745
- Enting I G and Mansbridge J V 1989 Seasonal sources and sinks of atmospheric CO₂: direct inversion of filtered data *Tellus* **41B** 111–26
- Enting I G and Mansbridge J V 1991 Latitudinal distribution of sources and sinks of CO₂: results of an inversion study *Tellus, Ser. B* **43** 156–70
- Enting I G, Trudinger C M and Francey R J 1995 A synthesis inversion of the concentration and $\delta^{13}\text{C}$ of atmospheric CO₂ *Tellus, Ser. B* **47** 35–52
- Eyers C J, Norman P, Middel J, Plohr M, Michot S, Atkinson K and Christou R A 2005 AERO2k Global Aviation Emissions Inventories for 2002 and 2025, QinetiQ/04/001113
- Folberth G, Hauglustaine D A, Ciais P and Lathière J 2005 On the role of atmospheric chemistry in the global CO₂ budget *Geophys. Res. Lett.* **32** L08801
- Gelaro R et al 2017 The Modern-era Retrospective Analysis for Research and Applications, version 2 (MERRA-2) *J. Clim.* **30** 5419–54
- Graven H et al 2018 Assessing fossil fuel CO₂ emissions in California using atmospheric observations and models *Environ. Res. Lett.* **13** 065007
- Guenther A 2000 Natural emissions of non-methane volatile organic compounds, carbon monoxide, and oxides of nitrogen from North America *Atmos. Environ.* **34** 2205–30
- Guenther A, Baugh B, Brasseur G, Greenberg J, Harley P, Klinger L, Serca D and Vierling L 1999 Isoprene emission estimates and uncertainties for the central African EXPRESSO study domain *J. Geophys. Res. Atmos.* **104** 30625–39
- Gurney K, Law R, Rayner P and Denning A S 2000 TransCom 3 Experimental Protocol, Department of Atmospheric Science, Colorado State University, USA, Paper 707. Available at: http://transcom.colostate.edu/TransCom_3/transcom_3.html
- Gurney K R, Chen Y-H, Maki T, Kawa S R, Andrews A and Zhu Z 2005 Sensitivity of atmospheric CO₂ inversions to seasonal and interannual variations in fossil fuel emissions *J. Geophys. Res.* **110** D10308
- Gurney K R et al 2002 Towards robust regional estimates of CO₂ sources and sinks using atmospheric transport models *Nature* **415** 626–30
- Gurney K R, Mendoza D, Zhou Y, Fischer M, de la Rue Du Can S, Geethakumar S and Miller C 2009 The Vulcan Project: high resolution fossil fuel combustion CO₂ emissions fluxes for the United States *Environ. Sci. Technol.* **43** 5535–41
- Houweling S et al 2015 An intercomparison of inverse models for estimating sources and sinks of CO₂ using GOSAT measurements *J. Geophys. Res. Atmos.* **120** 5253–66

- Imasu R 2019 Expected Scientific Achievement by GOSAT-2—Science Plan *J. Remote Sens. Soc. Japan* **39** 9–13
- IPCC 2019 *2019 Refinement to the 2006 IPCC Guidelines for National Greenhouse Gas Inventories*, ed E Calvo Buendia, K Tanabe, A Kranjc, J Baasansuren, M Fukuda, S Ngarize, A Osako, Y Pyrozhenko, P Shermanau and S Federici (Geneva: IPCC)
- Jacobson A R, Mikaloff Fletcher S E, Gruber N, Sarmiento J L and Gloor M 2007 A joint atmosphere-ocean inversion for surface fluxes of carbon dioxide: 2. Regional results, Glob. Biogeochem. Cycles **21** GB1020
- Kawa S R, Erickson D J III, Pawson S and Zhu Z 2004 Global CO₂ transport simulations using meteorological data from the NASA data assimilation system *J. Geophys. Res.* **109** D18312
- Lauvaux T et al 2016 High-resolution atmospheric inversion of urban CO₂ emissions during the dormant season of the Indianapolis Flux Experiment (INFLUX) *J. Geophys. Res.-Atmos.* **121** 5213–36
- Le Quéré C et al 2015 Global Carbon Budget 2015 *Earth Syst. Sci. Data* **7** 349–96
- Leip A, Skiba U, Vermeulen A and Thompson R L 2018 A complete rethink is needed on how greenhouse gas emissions are quantified for national reporting *Atmos. Environ.* **174** 237–40
- Liu J, Bowman K, Parazoo N C, Bloom A A, Wunch D, Jiang Z, Gurney K R and Schimel D 2018 Detecting drought impact on terrestrial biosphere carbon fluxes over contiguous US with satellite observations *Environ. Res. Lett.* **13** 095003
- Maksyutov S et al 2013 Regional CO₂ flux estimates for 2009–2010 based on GOSAT and groundbased CO₂ observations *Atmos. Chem. Phys.* **13** 9351–73
- Manning A J, O'Doherty S, Jones A R, Simmonds P G and Derwent R G 2011 Estimating UK methane and nitrous oxide emissions from 1990 to 2007 using an inversion modeling approach *J. Geophys. Res.* **116** D02305
- Nassar R, Hill T G, Mclinden C A, Wunch D, Jones D B A and Crisp D 2017 Quantifying CO₂ emissions from individual power plants from space *Geophysical Research Letters* **44** 10 045–53
- Nassar R et al 2010 Modeling global atmospheric CO₂ with improved emission inventories and CO₂ production from the oxidation of other carbon species *Geosci. Model Dev.* **3** 689–716
- Nielsen J et al 2017 Chemical mechanisms and their applications in the Goddard Earth Observing System (GEOS) earth system model *J. Adv. Model. Earth Syst.* **9** 3019–44
- Nivitanont J, Crowell S M R and Moore B III 2019 A scanning strategy optimized for signal-to-noise ratio for the Geostationary Carbon Cycle Observatory (GeoCarb) instrument *Atmos. Meas. Tech.* **12** 3317–34
- O'Dell C W et al 2012 The ACOS CO₂ retrieval algorithm Part 1: description and validation against synthetic observations *Atmos. Meas. Tech.* **5** 99–121
- Oda T and Maksyutov S 2011 A very high-resolution (1 km × 1 km) global fossil fuel CO₂ emission inventory derived using a point source database and satellite observations of nighttime lights *Atmos. Chem. Phys.* **11** 543–56
- Oda T and Maksyutov S 2015 ODIAC Fossil Fuel CO₂ Emissions Dataset, Center for Global Environmental Research, National Institute for Environmental Studies (<https://doi.org/10.17595/20170411.001>)
- Oda T, Maksyutov S and Andres R J 2018 The Open-source Data Inventory for Anthropogenic CO₂, version 2016 (ODIAC2016): a global monthly fossil fuel CO₂ gridded emissions data product for tracer transport simulations and surface flux inversions *Earth Syst. Sci. Data* **10** 87–107
- Oman L D, Douglass A R, Ziemke J R, Rodriguez J M, Waugh D W and Nielsen J E 2013 The ozone response to ENSO in Aura satellite measurements and a chemistry-climate simulation *J. Geophys. Res.* **118** 965–76
- Osterman G, Eldering A, Avis C, O'Dell C, Martinez E, Crisp D, Frankenberg C and Frankenberg B 2013 *ACOS Level 2 Standard Product Data User's Guide, V3.4* Jet Propulsion Laboratory, Pasadena, California
- Ott L E et al 2015 Assessing the magnitude of CO₂ flux uncertainty in atmospheric CO₂ records using products from NASA's Carbon Monitoring Flux Pilot Project *J. Geophys. Res. Atmos.* **120** 734–65
- Palmer P, Suntharalingam P, Jones D, Jacob D, Streets D, Fu Q, Vay S and Sachse G 2006 Using CO₂: CO correlations to improve inverse analyses of carbon fluxes *J. Geophys. Res.* **111** D12318
- Peylin P et al 2013 Global atmospheric carbon budget: results from an ensemble of atmospheric CO₂ inversions *Biogeosciences* **10** 6699–720
- Randerson J T, Thompson M V and Malmstrom C M 1996 Substrate limitations for heterotrophs: implications for models that estimate the seasonal cycle of atmospheric CO₂ *Global Biogeochem. Cycles* **10** 585–602
- Reuter M et al 2014 Satellite-inferred European carbon sink larger than expected *Atmos. Chem. Phys.* **14** 13739–53
- Rienecker M M et al 2011 MERRA: NASA's Modern-era Retrospective Analysis for Research and Applications *J. Climate* **24** 3624–48
- Gourdji S M, Yadav V, Karion A, Mueller K L, Conley S, Ryerson T, Nehr Korn T and Kort E A 2018 Reducing errors in aircraft atmospheric inversion estimates of point-source emissions: the Aliso Canyon natural gas leak as a natural tracer experiment *Environ. Res. Lett.* **13** 045003
- Strahan S E, Duncan B N and Hoor P 2007 Observationally derived transport diagnostics for the lowermost stratosphere and their application to the GMI chemistry and transport model *Atmos. Chem. Phys.* **7** 2435–45
- Suntharalingam P, Randerson J T, Krakauer N, Logan J A and Jacob D J 2005 Influence of reduced carbon emissions and oxidation on the distribution of atmospheric CO₂: implications for inversion analyses *Global Biogeochem. Cycles* **19** GB4003
- Takagi H et al 2011 On the benefit of GOSAT observations to the estimation of regional CO₂ fluxes *Sci. Online Lett. Atmos.* **7** 161–4
- Takahashi T et al 2009 Climatological mean and decadal change in surface ocean pCO₂, and net sea-air CO₂ flux over the global oceans *Deep Sea Res., Part II* **56** 554–77
- Tsutsumi Y, Mori K, Ikegami M, Tashiro T and Tsuboi K 2006 Long-term trends of greenhouse gases in regional and background events observed during 1998–2004 at Yonagunijima located to the east of the Asian continent *Atmos. Environ.* **40** 5868–79
- van der Werf G R, Randerson J T, Giglio L, Collatz G J, Kasibhatla P S and Arellano A F Jr. 2006 Interannual variability in global biomass burning emissions from 1997 to 2004 *Atmos. Chem. Phys.* **6** 3423–41
- van der Werf G R, Randerson J T, Giglio L, Collatz G J, Mu M, Kasibhatla P S, Morton D C, Defries R S, Jin Y and van Leeuwen T T 2010 Global fire emissions and the contribution of deforestation, savanna, forest, agricultural, and peat fires (1997–2009) *Atmos. Chem. Phys.* **10** 11707–35
- Wang J S, Kawa S R, Collatz G J, Sasakawa M, Gatti L V, Machida T, Liu Y and Manyin M E 2018 A global synthesis inversion analysis of recent variability in CO₂ fluxes using GOSAT and in situ observations *Atmos. Chem. Phys.* **18** 11097–124
- Wang J S, Logan J A, McElroy M B, Duncan B N, Megretskaya I A and Yantosca R M 2004 A 3-D model analysis of the slowdown and interannual variability in the methane growth rate from 1988 to 1997 *Global Biogeochem. Cycles* **18** GB3011